

Fusion Reactor Technology 2

(459.761, 3 Credits)

Prof. Dr. Yong-Su Na

(32-206, Tel. 880-7204)

Operation Limits

- **Density ranges in a tokamak discharge**
 - There exist a lower and an upper density limit at a given I_p .
- **Low densities**
 - e-i collision frequency not sufficient to prevent the generation of run-away or accelerated electrons
 - run-away electrons produced by the inductive E field
 - run-away electrons spoil the discharge characteristics and may be dangerous for the vacuum chamber
- **High densities**
 - atomic processes (radiation, CX, neutral atom ionization) at the plasma edge become rather important
 - atomic processes can lead to contraction of the plasma column (decrease of the effective plasma radius)
 - danger of kink instability becomes real

Operation Limits

- **Assumptions**

- Circular CX, steady-state with purely OH heating, $T_e = T_i = T$, no impurities, atomic processes not important (radiation, recycling, etc), fully ionized hot plasma
- Under these conditions, one can expect the existence of self-similar self-organized plasma states, if they have the same macroscopic non-dimensional parameters.

Operation Limits

- **Murakami and Hugill Numbers**

- consider atomic processes

$$a, R, B_T, B_p, m_e, m_i, e, n, T$$

- To evaluate the role of atomic processes appropriate power losses with Joule heating power should be compared.

$$P_{OH} = \eta j^2 = \frac{m_e v_{ei}}{ne^2} \left(\frac{B_T}{\mu_0 q_a R} \right)^2 = \frac{L \hbar^3}{m_e e^4} F(T_*) \frac{B_T^2}{\mu_0^2 q_a^2 R^2}$$

$$T_* = T / \varepsilon_a \quad r_a = \frac{\hbar^2}{m_e e^2}, \quad v_a = \frac{e^2}{\hbar}, \quad \varepsilon_a = \frac{m_e e^4}{\hbar^2}$$

$L \sim 12.3$ Coulomb logarithm

Introduce atomic units for length, velocity, energy

$$P_R = n^2 r_a^2 v_a \varepsilon_a G(T_*) = n^2 \frac{e^2 \hbar}{m_e} G(T_*)$$

Losses due to radiation and ionization

Dimensional Analysis of Tokamaks

- If P_R becomes comparable to P_{OH} , atomic processes start to play a significant role.

$$P_R / P_{OH} = H^2 G(T_*) / F(T_*) \quad H = \frac{e \gamma n q_a R}{B_T \sqrt{L}}, \quad \gamma = \frac{e^2}{\hbar c}$$

- The role of atomic processes is defined by a non-dimensional parameter H (Hugill number): as increasing H , the role of atomic processes increases compared with OH heating

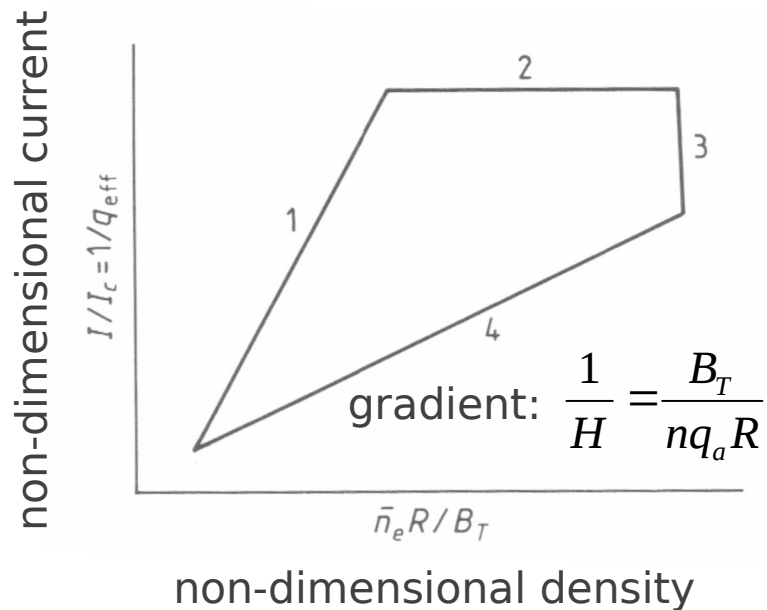
$$H = \frac{n q_a R}{B_T} \quad \text{if } L = 12.3$$

$$M = \frac{n R}{B_T} \quad \text{Murakami number}$$

Operation Limits

- **Hugill plot**

- limited operational region on the current-density plane
- non-dimensional current .VS. non-dimensional density



$$q_a = \frac{aB_T}{RB_p} = \frac{aB_T}{R\mu_0 I / 2\pi a} = \frac{2\pi a^2 B_T}{\mu_0 IR}$$

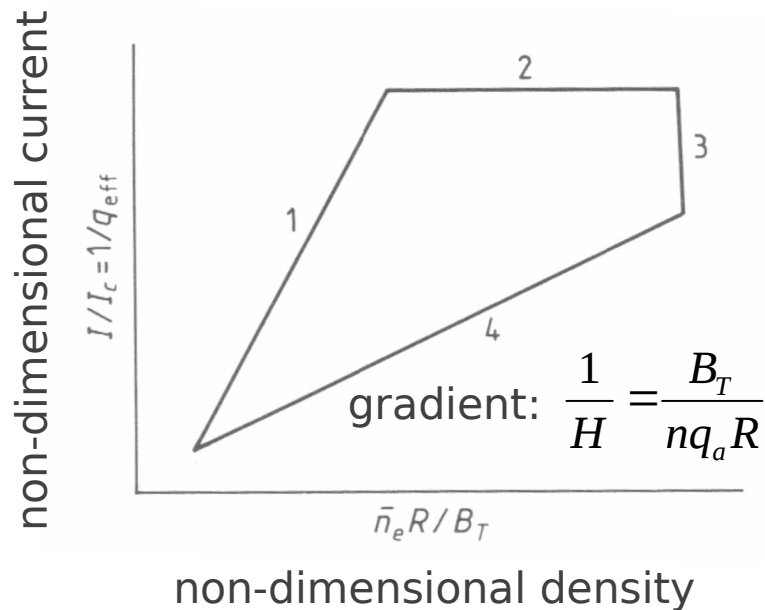
$$\frac{1}{q_a} = \frac{I}{2\pi a^2 B_T / \mu_0 R} = \frac{I}{I_c}$$

$$M = \frac{\bar{n}R}{B_T} \quad \text{Murakami number}$$

Operation Limits

- **Hugill plot**

- Tokamak operational domain on the current-density plane is restricted by four limits.



1: limit of run-away electrons at

low density $j / en = v_e^{\text{thermal}} = \sqrt{2T / m_e}$

2: current limit due to the MHD-instability

3: Murakami limit at high density (at the maximal permissible plasma current): radiative power balance

4: Hugill density limit where H ($H = q_{\text{eff}} M$) remains constant ($n \sim I$): confinement/disruptive limit

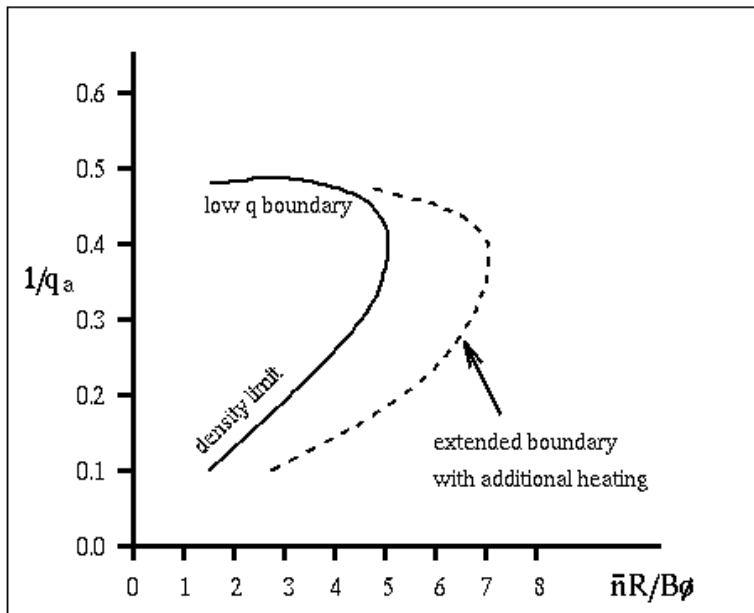
- The limiting density is determined by the power balance on the plasma periphery (by balance of the energy flow from the central region and radiation and ionization losses).

- The density limit usually increases with additional heating as $P^{1/2}$.

Operation Limits

- **Hugill plot**

- Tokamak operational domain on the current-density plane is restricted by four limits.



- 1: limit of run-away electrons at

low density $j/en = v_e^{thermal} = \sqrt{2T/m_e}$

- 2: current limit due to the MHD-instability

- 3: Murakami limit at high density (at the maximal permissible plasma current): radiative power balance

- 4: Hugill density limit where H ($H = q_{eff}M$) remains constant ($n \sim I$): confinement/disruptive limit

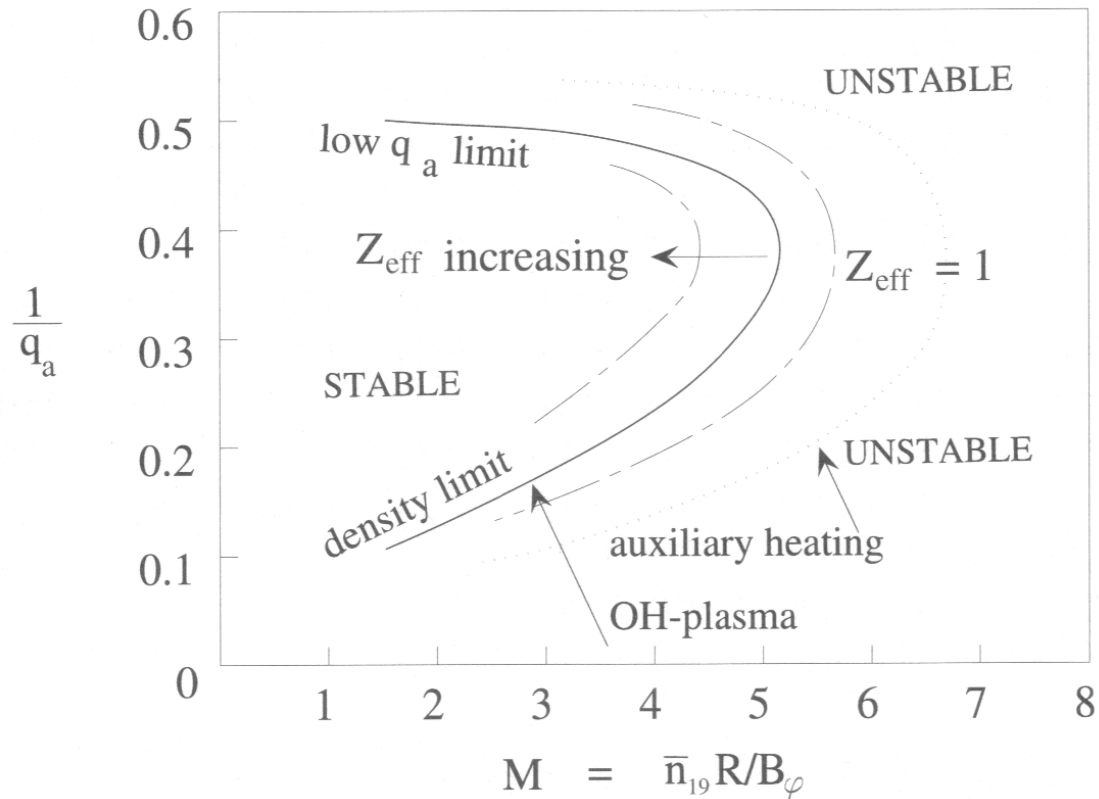
- The limiting density is determined by the power balance on the plasma periphery (by balance of the energy flow from the central region and radiation and ionization losses).

- The density limit usually increases with additional heating as $P^{1/2}$.

Operation Limits

- **Hugill plot**

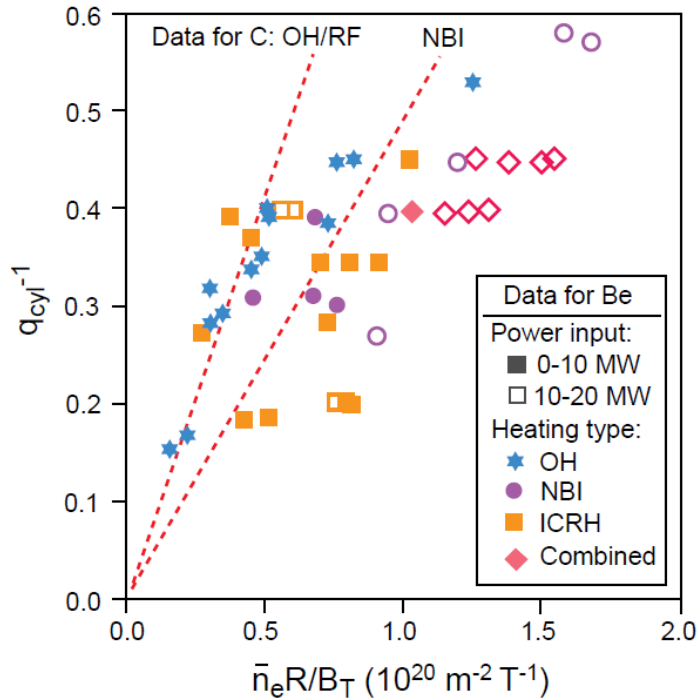
- limited operational region on the current-density plane
- non-dimensional current .VS. non-dimensional density



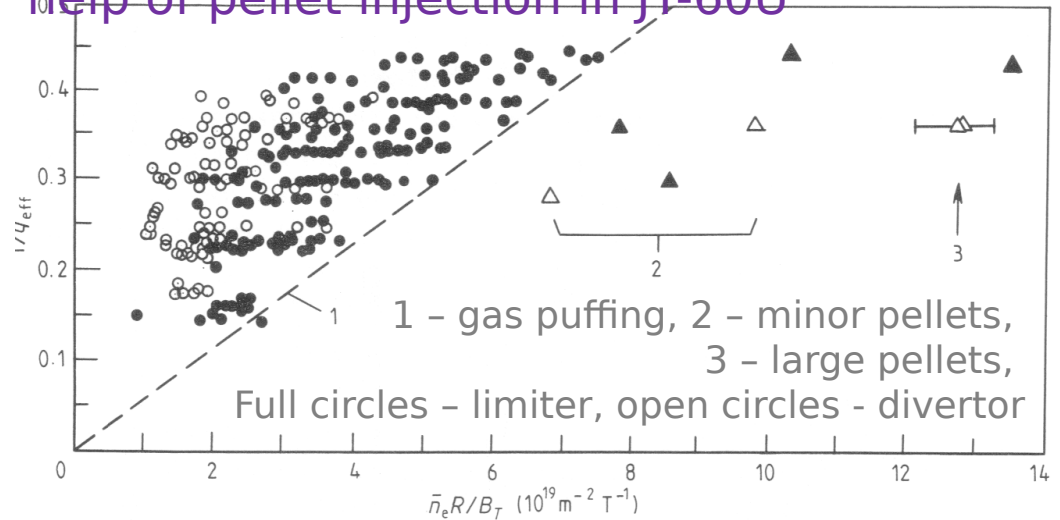
Operation Limits

- **Hugill plot**

- Attaining high densities by using beryllium coating of the chamber



help of pellet injection in JT-60U



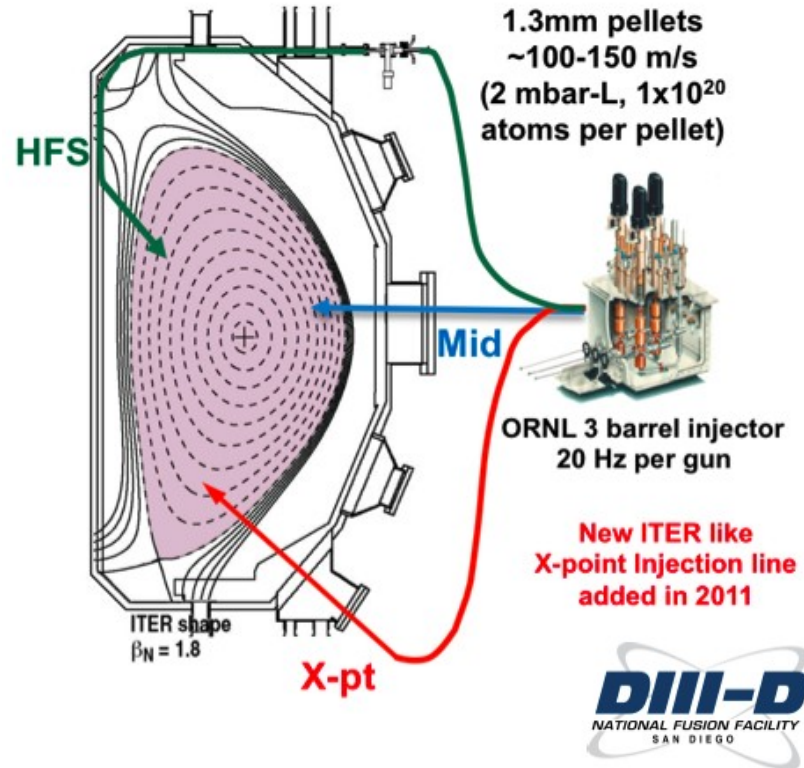
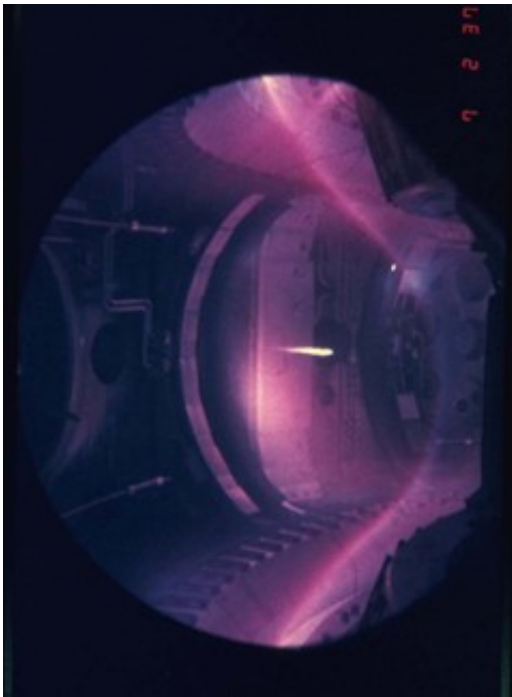
- The two dashed lines illustrate the density limits in earlier OH/ICRF and NBI experiments with a mainly carbon 1st wall.
- When heating power is increased, the Hugill limit shifts towards higher densities.

Operation Limits

- **Hugill plot**

- Attaining high densities by using beryllium coating of the chamber wall in JET and with the help of pellet injection in JT-60U

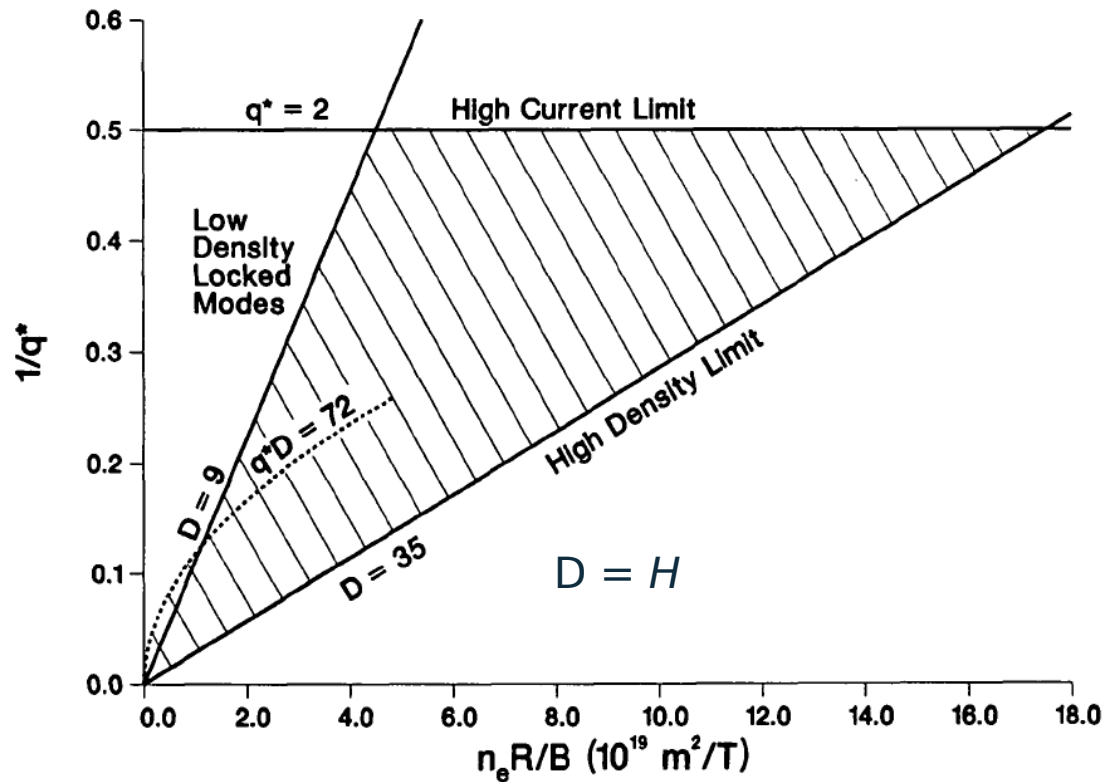
- wall in JET and with the help of pellet injection in JT-60U



Operation Limits

- **Hugill plot**

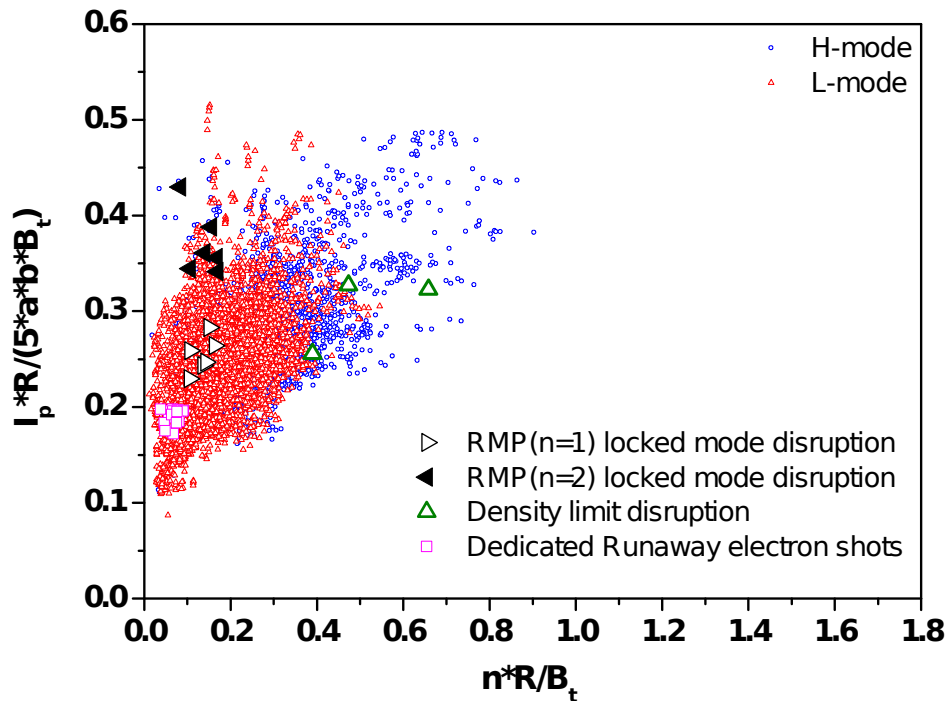
- limited operational region on the current-density plane
- non-dimensional current .VS. non-dimensional density



Operation Limits

- **Hugill plot**

- limited operational region on the current-density plane
- non-dimensional current .VS. non-dimensional density



Operation Limits

- Greenwald density limit

$$q_a = \frac{aB_T}{RB_p} = \frac{aB_T}{R\mu_0 I / 2\pi a} = \frac{2\pi a^2 B_T}{\mu_0 IR}$$

$$\frac{1}{q_a} = \frac{\mu_0 IR}{2\pi a^2 B_T} \approx \frac{M}{15} = \frac{\bar{n}R}{15B_T}$$

$$\bar{n}_{20} \approx \frac{I}{\pi a^2} \quad \text{Greenwald limit}$$

- For stability observations yield the conditions

$$\bar{n}_{20} \leq \frac{I}{\pi a^2}, \quad q_a > 2$$

Basic Tokamak Variables

- Greenwald density

$$\bar{n} = \kappa \bar{J} \quad (1)$$

measured in 10^{20} m^{-3} , where κ is the plasma elongation and \bar{J} is the average plasma current density, with the I_p area measured in $\text{MA} \cdot \text{m}^{-2}$. Figures 4a to 4d are modified Hugill plots for several machines, showing the results of this scaling. They should be compared with Fig. 3. For elliptical machines this scaling for the density limit can be written as $\bar{n}_{\text{max}} = I_p / \pi a^2$, and for high aspect ratio, low beta, circular machines it can be written as $(5/\pi) \times B/qR$. A few comments on

A NEW LOOK AT DENSITY LIMITS IN TOKAMAKS

M. GREENWALD, J.L. TERRY, S.M. WOLFE

Plasma Fusion Center,
Massachusetts Institute of Technology,
Cambridge, Massachusetts

S. EJIMA*

General Atomic Technologies,
San Diego, California

M.G. BELL, S.M. KAYE

Princeton Plasma Physics Laboratory,
Princeton University,
Princeton, New Jersey

G.H. NEILSON

Oak Ridge National Laboratory,
Oak Ridge, Tennessee

United States of America

ABSTRACT. While the results of early work on the density limit in tokamaks from the ORMAK and DITE groups have been useful over the years, results from recent experiments and the requirements for extrapolation to future experiments have prompted a new look at this subject. There are many physical processes which limit the attainable densities in tokamak plasmas. These processes include: (1) radiation from low Z impurities, convection, charge exchange and other losses at the plasma edge; (2) radiation from low or high Z impurities in the plasma core; (3) deterioration of particle confinement in the plasma core; and (4) inadequate fuelling, often exacerbated by strong pumping by walls, limiters or divertors. Depending upon the circumstances, any of these processes may dominate and determine a density limit. In general, these mechanisms do not show the same dependence on plasma parameters. The multiplicity of processes leading to density limits with a variety of scaling has led to some confusion when comparing density limits for different machines. The authors attempt to sort out the various limits and to extend the scaling law for one of them to include the important effects of plasma shaping, i.e. $\bar{n}_e = \kappa \bar{J}$, where \bar{n}_e is the line average electron density (10^{20} m^{-3}), κ is the plasma elongation and \bar{J} ($\text{MA} \cdot \text{m}^{-2}$) is the average plasma current density, defined as the total current divided by the plasma cross-sectional area. In a sense, this is the most important density limit since, together with the q-limit, it yields the maximum operating density for a tokamak plasma. It is shown that this limit may be caused by a dramatic deterioration in core particle confinement occurring as the density limit boundary is approached. This mechanism can help explain the disruptions and Marfes that are associated with the density limit.

Basic Tokamak Variables

- **Greenwald density**

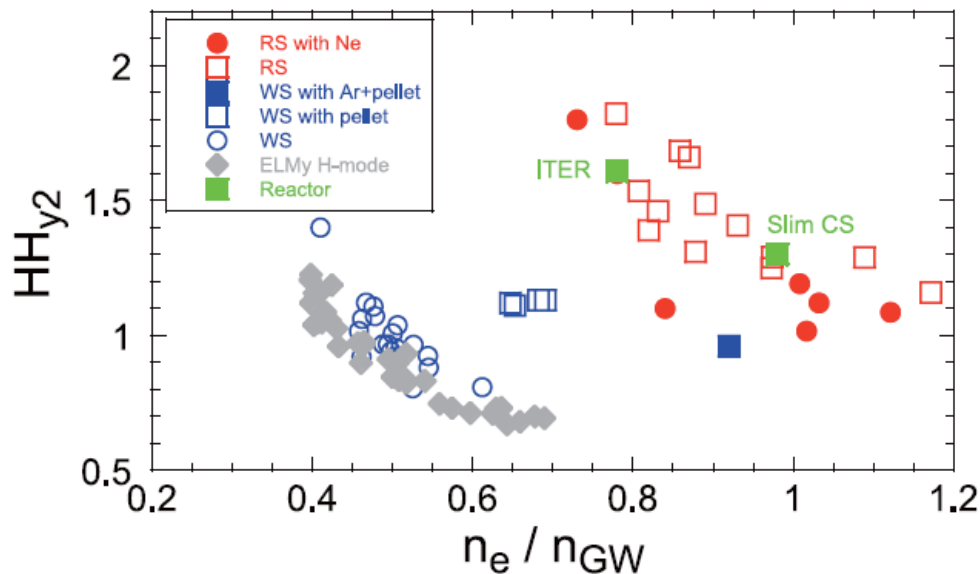
$$n_G = \frac{I_p}{\pi a^2}$$

- As the limit is approached, the plasma becomes increasingly susceptible to disruption and data become sparser.

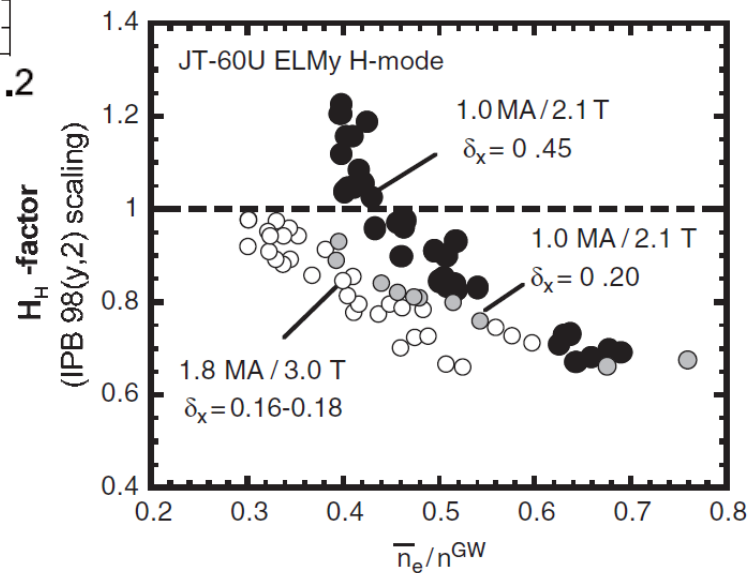
*M. Greenwald et al, NF **28** 199 (1988): one of the most cited paper in NF
Martin Greenwald, PPCF **44** R27 (2002)*

Basic Tokamak Variables

- Greenwald density



Y. Sakamoto et al, PFR **5** S1008 (2010)
 H. Urano et al, PPCF **44** 11 (2002)



Operation Limits

- **Pressure Limit**

- related to the ballooning instability occurring due to convex magnetic lines of the outer region: swelling on magnetic surface at the high pressures
- force balance between the cause for swelling (plasma pressure gradient) and the magnetic tension

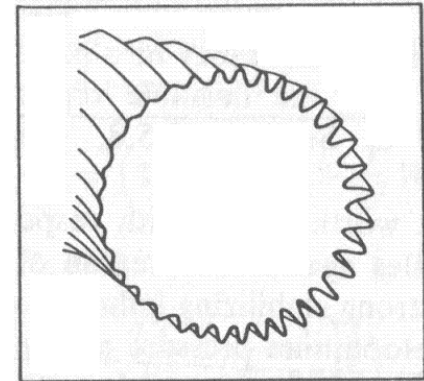
$$\frac{p}{a} = \frac{B_T^2}{2\mu_0 q R}$$

$$\beta_c = \frac{p}{B_T^2 / 2\mu_0} = \frac{a}{qR} = \frac{a}{2\pi\kappa a^2 B_T R / \mu_0 I R}$$

$$= g \frac{I}{a B_T} \equiv g I_N$$

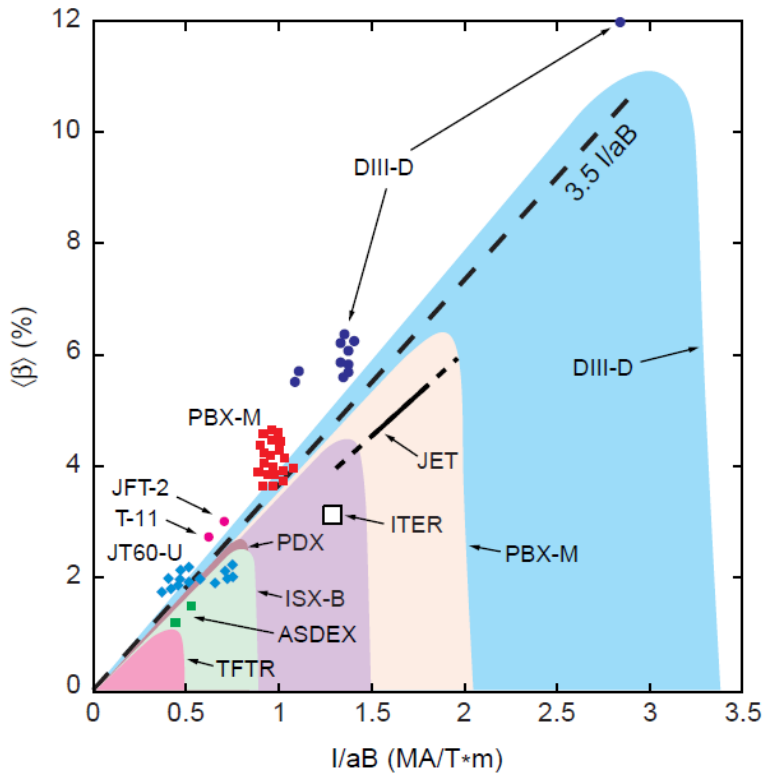
$g = \beta_N$: Troyon factor

$$I_N = \frac{I}{a B_T} = \frac{I}{I_c} \frac{2\pi\kappa a}{\mu_0 R} \quad q = \frac{2\pi\kappa a^2 B_T}{\mu_0 I R} = \frac{I_c}{I}$$

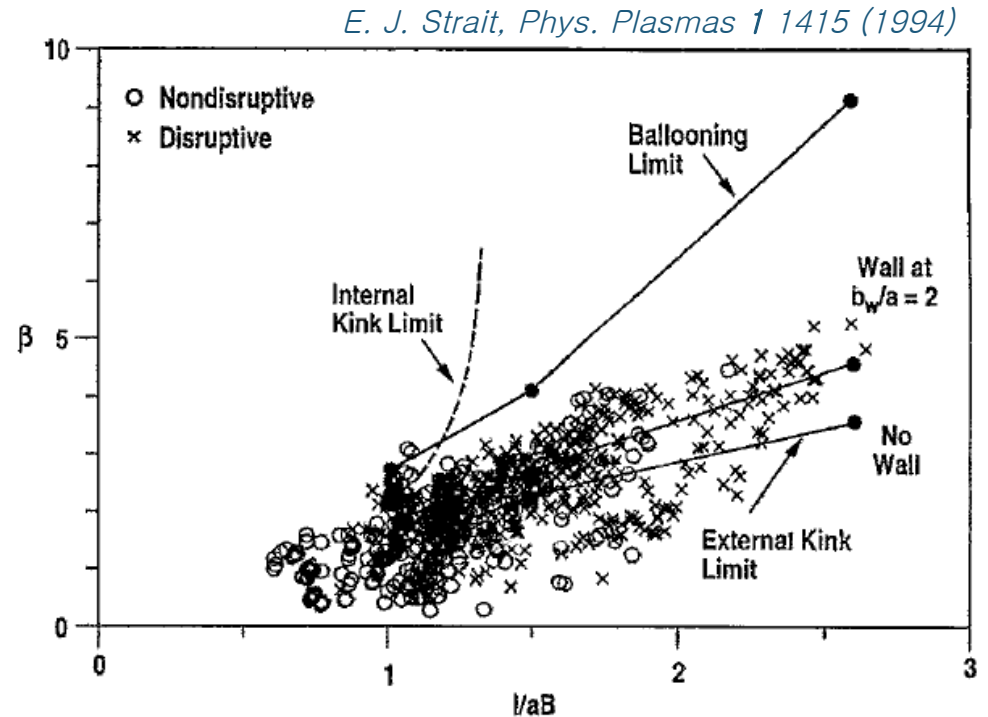


Operation Limits

$$\beta_c = \beta_N \frac{I}{aB_T}$$



ITER Physics Basis, Nuclear Fusion 39 2261 (1999)



E. J. Strait, Phys. Plasmas 1 1415 (1994)

Operating range of high beta discharges in PBX compared to calculated stability limits, including the ideal $n = 1$ external kink limit with a conducting wall at twice the plasma minor radius and without a wall

Operation Limits

- **Pressure Limit**

- If g is constant, for the most effective use of the B_T it is preferable to have the values of β as high as possible.

→ high I_N

$$\beta_c = g I_N = g \frac{I}{I_c} \frac{2\pi\kappa a}{\mu_0 R}$$

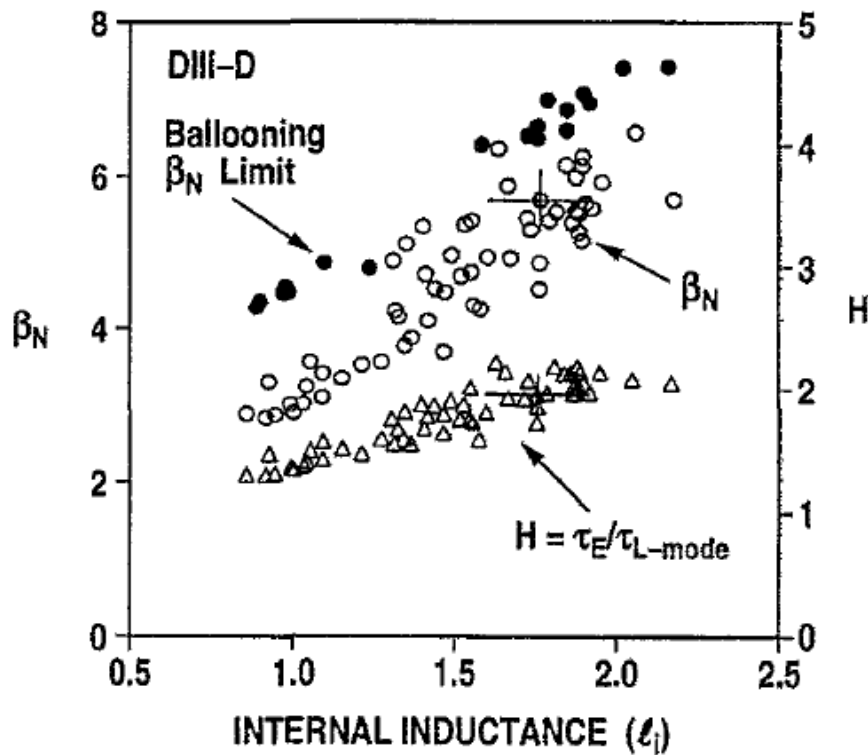
- Since I/I_c is limited by the upper current limit on the Hugill diagram, $\kappa a/R$ should be maximized.

→ The column should be elongated vertically as much as possible.

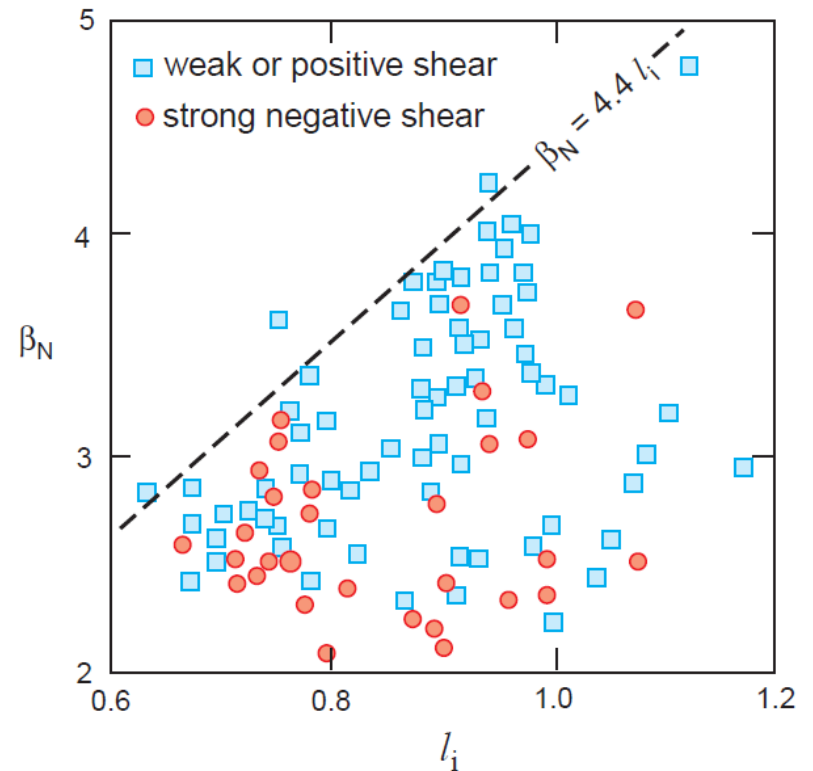
- The experimental data for critical β are summarized by a simple empirical formulae $\beta_c = \beta_N \frac{I}{aB_T} = 4l_i \frac{I}{aB_T}$

Operation Limits

$$\beta_N \approx 4l_i$$



E. J. Strait, Phys. Plasmas 1 1415 (1994)



ITER Physics Basis, Nuclear Fusion 39 2261 (1999)

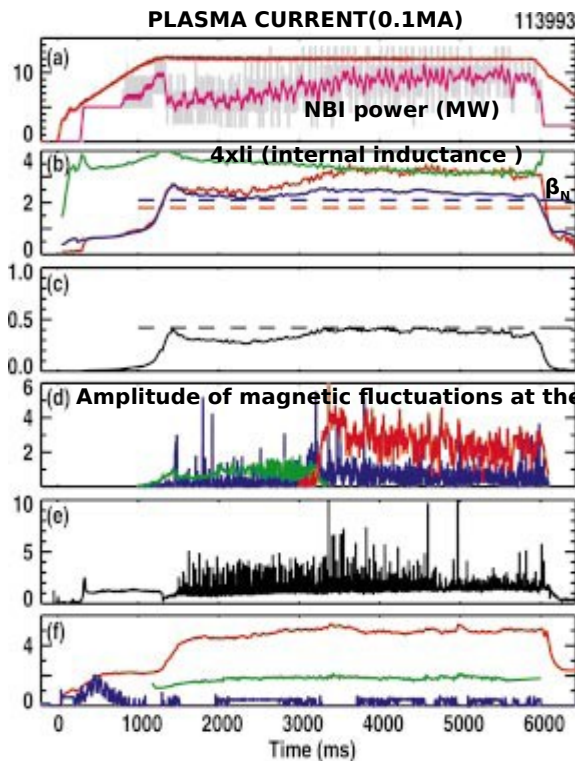
Operation Limits

- DIII-D hybrid modes

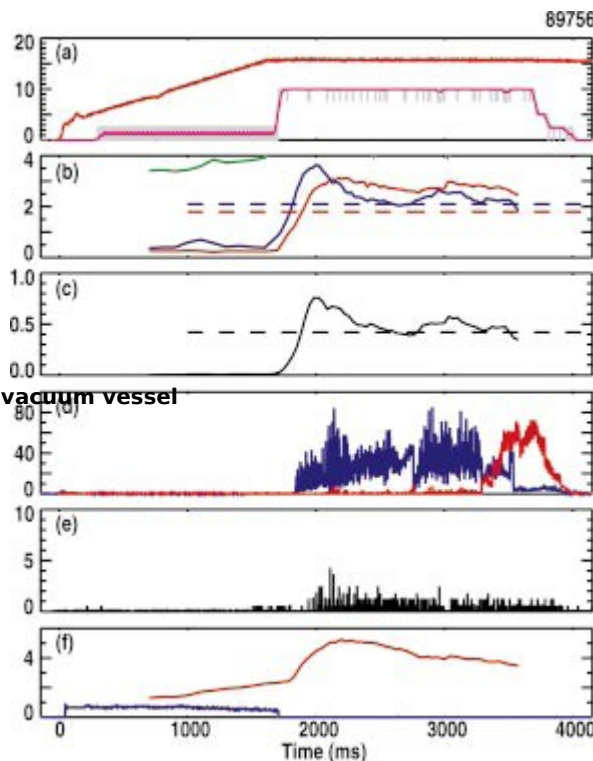
$q_{95} > 4$ without sawteeth

$q_{95} = 3.6$ without sawteeth

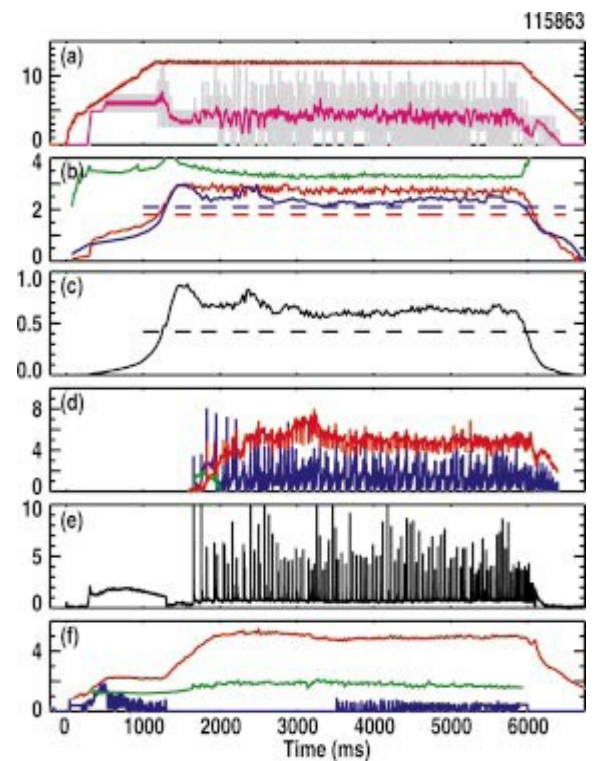
$q_{95} = 3.2, \beta_N = 2.7, H_{89P} = 2.3$



limited by tearing modes



limited by fishbones

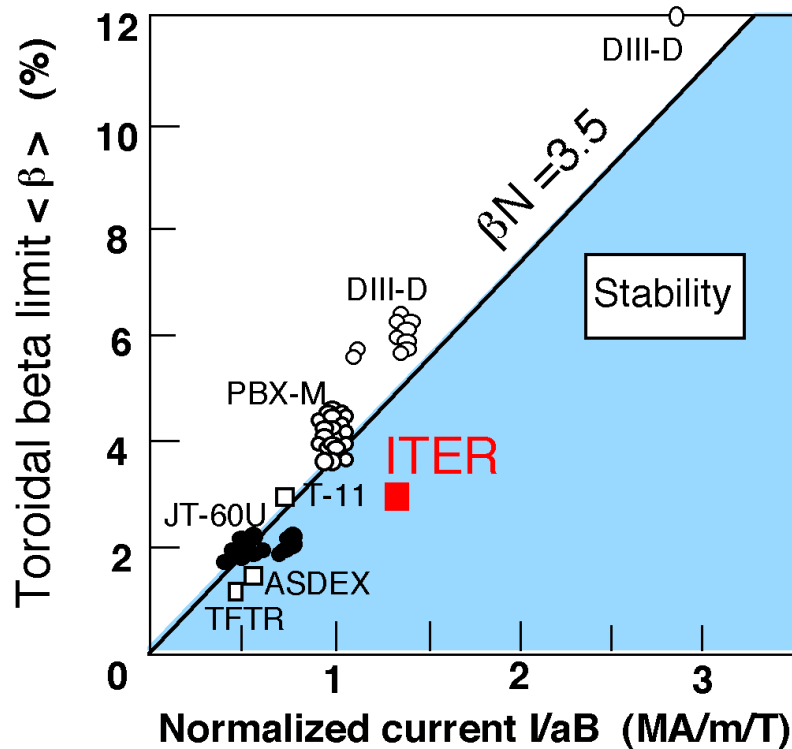


limited by sawteeth

Operation Limits

- Pressure Limit

$$\beta_N = \beta_t \frac{aB_t}{I_p}$$

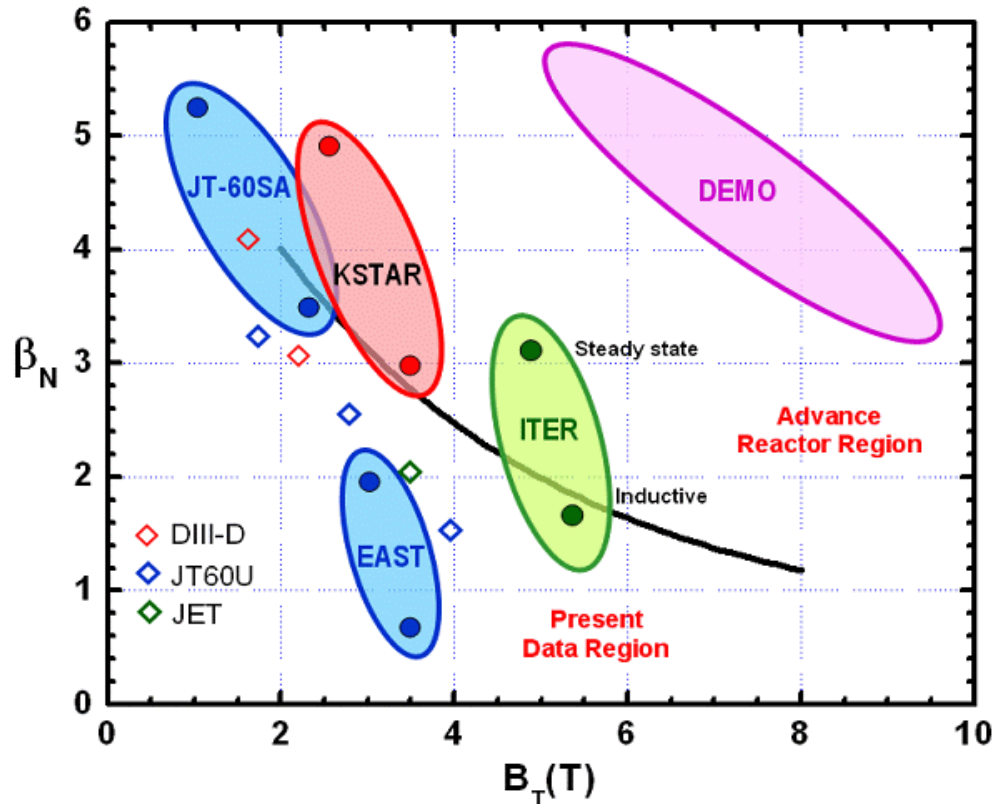


- Fundamental elements affecting the β_N -limit

1. Current profile
2. Pressure profile
3. Plasma shape
4. Stabilising wall

Operation Limits

- Pressure Limit



- High β_N in KSTAR
1. Strong plasma shaping (PF/CS system capability)
 2. Passive stabilizers
 3. High heating power
 4. RWM control coils

